



Exploration of Synthesis and Electrical Properties of $\text{Ni}_{0.1}\text{Mn}_{0.4}\text{Cu}_{0.2}\text{Cd}_{0.3}\text{Fe}_2\text{O}_4$ Produced by Sol-Gel Auto Combustion Procedure

M. Moazzam Hossen*

*Department of Computer Science and Engineering, International Islamic University Chittagong, Chattogram
4318, Bangladesh*

Email: moazzam.physics@gmail.com

Abstract

$\text{Ni}_{0.1}\text{Mn}_{0.4}\text{Cu}_{0.2}\text{Cd}_{0.3}\text{Fe}_2\text{O}_4$ has been planned to prepare by the sol-gel auto combustion procedure. From the frequency 20 Hz to the frequency 15 MHz, dielectric properties, electric modulus, impedance spectroscopy, and ac conductivity has been documented with the help of an impedance analyzer. From the graph of the real dielectric part, it has been viewed that the dielectric constant value reduces with the boost of frequency that can be elucidated through Maxwell and Wagner's two-layer theory. A lucid peak has been found in the graph of the imaginary electric modulus part that is the clear distinction between two conduction regions in the frequency area. In the impedance spectroscopy, high impedance has been monitored in the low-frequency section. Enhance of ac conductivity in the high-frequency section reveals the activity of grains over grain boundary.

Keywords: Nanomaterials; Sol-Gel auto combustion procedure; Dielectric; Electric modulus; Impedance spectrum; AC conductivity.

1. Introduction

From the application and research view, among all the magnetic materials that can be functional in recent electronic functions, spinel ferrites are the most fascinating one.

* Corresponding author.

Recently, these spinel ferrites are extensively utilized in the microwave and electrical industries due to their unique electric properties that also diverge a lot from their bulk counterpart. Ferrite exhibits elevated resistivity value and small eddy current losses that are useful for high-frequency uses. In the world of nanotechnology, spinel ferrites have been able to create attention because of its size that is within the nano-range and its more substantial surface to volume ratio [1]. Within the soft ferrites, nickel-based ferrites can be used for commercial purpose as it possesses significant electrical properties. This sort of ferrites can be widely utilized as transformers, computer memories, inductors, and phase shifters. The consequence of constituents and temperature on the electrical characteristics of Ni-based ferrites has been extensively examined [2]. In addition, manganese-based ferrites that belong to the transition metal group possess high magnetic permeability and low losses along with numerous eminent dedicated purposes. Mn-based ferrites can be broadly utilized in computer memory chips, microwave devices, transformer cores, and magnetic recording media [3]. The existence of different chemical compositions in the material controls the intrinsic electric properties, whereas the synthesis technique controls the extrinsic electrical properties. To enhance the physical properties of ferrite materials, chemical elements and synthesis technique plays a vital role. To prepare spinel nano ferrites, there are various physical and chemical synthesis techniques, namely Hydrothermal [4], Co-precipitation [5], Combustion [6], Sol-gel [7]. In the typical method, the higher sintering temperature is needed that gives rise to the intergranular and intragranular porosity that, in turn, affect properties of the material. Apart from this limitation, the sol-gel auto combustion method provides different advantages by using low sintering temperatures such as high purity, ultrafine, and homogeneous particles for high-frequency applications. Shirsath and his colleagues [8] synthesized $\text{Ni}_{0.5-x}\text{Mn}_x\text{Zn}_{0.5}\text{Fe}_2\text{O}_4$ by the sol-gel auto-combustion process and sintered at 600 °C for 4h. They observed an enhancement in initial permeability with the raise of manganese proportion and then watched a decrease with further substitution of Mn proportion. Farooq and his colleagues [9] reproducibly synthesized manganese nano ferrites by the co-precipitation method. They have found the change in structural and dielectric characteristics with the alteration of the sintering temperature and time. They have measured dielectric constant at room temperature from 600Hz to 1MHz by means of an LCR meter to notice the change in dielectric constant in both low and high-frequency range. Kumar and his colleagues [10] synthesized $\text{Ni}_{0.6}\text{Zn}_{0.4}\text{Gd}_y\text{Fe}_{2-y}\text{O}_4$ by low-temperature citrate gel auto-combustion process. They have been observed that with the substitution of gadolinium, dielectric constant increases almost five times. They also investigated the outcome of the grain periphery on the physical properties. For high-frequency applications, $\text{Ni}_{0.1}\text{Mn}_{0.4}\text{Cu}_{0.2}\text{Cd}_{0.3}\text{Fe}_2\text{O}_4$ nano ferrites draw more attention as a potential contestant. In the current research, $\text{Ni}_{0.1}\text{Mn}_{0.4}\text{Cu}_{0.2}\text{Cd}_{0.3}\text{Fe}_2\text{O}_4$ has been chosen to study the electrical properties. Until now, no structured reports have been published regarding the electrical properties of $\text{NiMnCuCdFe}_2\text{O}_4$. Hence, we aim to synthesize $\text{Ni}_{0.1}\text{Mn}_{0.4}\text{Cu}_{0.2}\text{Cd}_{0.3}\text{Fe}_2\text{O}_4$ nanoparticles by means of a sol-gel auto combustion procedure. Dielectric properties are sturdily correlated with Maxwell Wagner methods, and primarily we have focused our attention on that point along with other electric properties, namely electric modulus, impedance spectroscopy, and ac conductivity.

2. Experimental Procedures

2.1. Synthesis of nanoparticles

Taking salts of nickel nitrate ($\text{Ni}(\text{NO}_3)_2 \cdot 6\text{H}_2\text{O}$), manganese nitrate ($\text{Mn}(\text{NO}_3)_2 \cdot 6\text{H}_2\text{O}$), copper nitrate ($\text{Cu}(\text{NO}_3)_2 \cdot 3\text{H}_2\text{O}$), cadmium nitrate ($\text{Cd}(\text{NO}_3)_2 \cdot 4\text{H}_2\text{O}$), and ferric nitrate ($\text{Fe}(\text{NO}_3)_3 \cdot 9\text{H}_2\text{O}$) as the starting material, $\text{Ni}_{0.1}\text{Mn}_{0.4}\text{Cu}_{0.2}\text{Cd}_{0.3}\text{Fe}_2\text{O}_4$ nanoparticles has been produced by means of sol-gel auto ignition system. Initially a standardized combination was ready by liquefying the unrefined resources in ethanol ($\text{C}_2\text{H}_6\text{O}$). For two hours, the suspension was stimulated incessantly via means of a magnetic agitator. Concurrently, liquor ammonia was placed into the suspension drop-wise to sustain the pH of the solution at a rigid value 7. It took approximately twenty four hours to twist the solution into gel form entirely at temperature 80°C in a water bath. To obtain fluffy powder, the gel was warmed at 200°C for five hours in the air. This feathery powder was annealed at 700°C for five hours to attain final Ni-Mn-Cu-Cd nano-ferrites powder.

2.2. Characterization

To the value of ϵ' and ϵ'' have been approximated through the next law:

$$\epsilon' = \frac{Cd}{\epsilon_0 A} \dots\dots\dots (1)$$

where C-capacitance, d-pallet width, A- pallet’s cross-sectional area, ϵ_0 -free space’s permittivity.

The value of $\tan \delta$ has been found by the equation:

$$\tan \delta = \frac{\epsilon''}{\epsilon'} \dots\dots\dots (2)$$

All electrical properties have been recorded by Waynekerr impedance analyzer (model No. 6500B) at room temperature for the same frequency range.

3. Results and discussion

3.1. Dielectric Properties

The variation of ϵ' and ϵ'' with the frequency of $\text{Ni}_{0.1}\text{Mn}_{0.4}\text{Cu}_{0.2}\text{Cd}_{0.3}\text{Fe}_2\text{O}_4$ has been given in Figure 1 (a) and Figure 1 (b). It has been perceived from the graphs that with the increase of frequency, both ϵ' and ϵ'' decreases. The polarizing effect can explain this decreasing behavior. At low frequencies, the electron hopping conduction system can trail the electric field. At the same time, it becomes incapable of chasing the applied electric field at higher frequency range consequences drop in dielectric constant. This occurrence can also be construed by Koop's theory and Maxwell Wagner's interfacial polarization theory [11, 12]. Along the lines of this theory, at low frequency, the dielectric constant is as a consequence of the accretion of charges at the grain boundary where the value of resistance is elevated, whereas at high frequency, the dielectric constant produced from grains where the value of resistance is relatively inferior. An analogous sort of occurrence has been noticed by other researchers in the case of spinel ferrites [13]. The distinction in $\tan\delta$ with frequency has been given in Figure 1 (c). It has been monitored that the value of $\tan\delta$ decreases as the frequency expands. Conduction system also organizes straightly in the value of $\tan\delta$. Peaking in the $\tan\delta$ spectrum is watched when the hopping

frequency harmonized well with the exterior applied field [14].

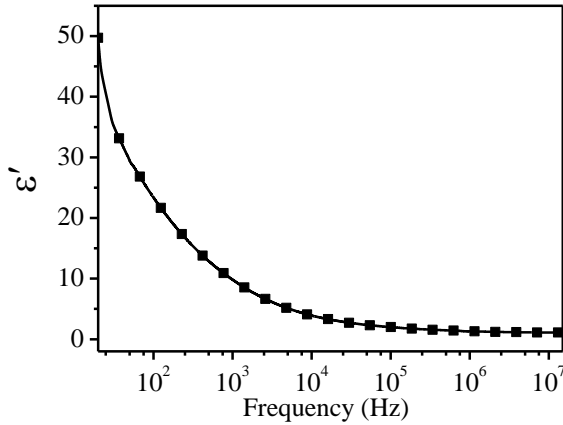


Figure 1(a): Variation of real parts of dielectric constant as a function of frequency in $\text{Ni}_{0.1}\text{Mn}_{0.4}\text{Cu}_{0.2}\text{Cd}_{0.3}\text{Fe}_2\text{O}_4$ nanoparticles

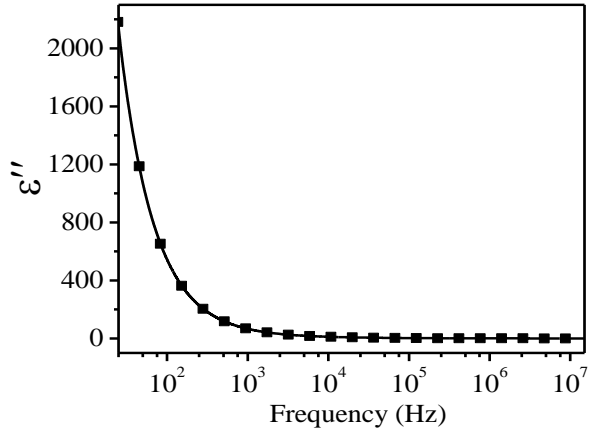


Figure 1(b): Variation of imaginary parts of dielectric constant as a function of frequency in $\text{Ni}_{0.1}\text{Mn}_{0.4}\text{Cu}_{0.2}\text{Cd}_{0.3}\text{Fe}_2\text{O}_4$ nanoparticles

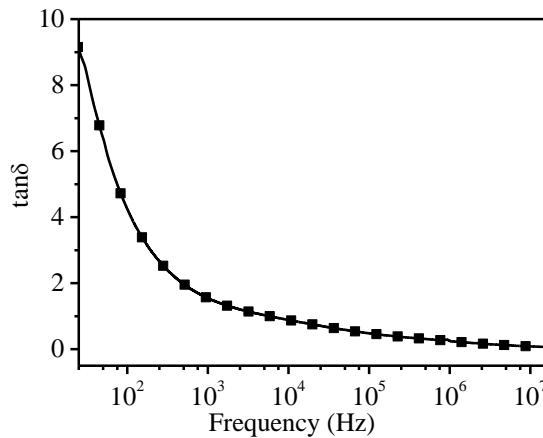


Figure 1(c): Variation of dielectric dissipation with log frequency for $\text{Ni}_{0.1}\text{Mn}_{0.4}\text{Cu}_{0.2}\text{Cd}_{0.3}\text{Fe}_2\text{O}_4$ ferrites nanoparticles

3.2. Electric Modulus

The real part (M') of the electric modulus of $\text{Ni}_{0.1}\text{Mn}_{0.4}\text{Cu}_{0.2}\text{Cd}_{0.3}\text{Fe}_2\text{O}_4$ has been shown in Figure 2 (a). In the low-frequency constituency, which is below 10^2 Hz, the M' value is approaching zero. With ascends of frequency, this M' value augments up to the peak position saturation in the high-frequency region, which is superior to 10^2 Hz. This highest value of M' is as a consequence of space alteration of charge carriers in the short-range region in the conduction procedure. On the contrary, the minor value is as a result of the space alteration of charge carriers in the long-range province in the conduction procedure. The change of the imaginary part (M'') of electric modulus with frequency has been shown in Figure 2 (b). A lucid crest has been monitored in the figure that divides the whole frequency region into two regions. In the low-frequency province, the charge carriers can jump among two closes by sites that outcome in long-range mobility. Whereas in the high-frequency province, the reverse incident takes place, where charge carriers are only can steps forward

within a short-range. With the increase of frequency, these distinctive crests give crucial information about the category of mobility that occurs in the structure [15]. The complex modulus plot (M'' versus M') at various compositions has been given in Figure 2 (c). Well-resolved semicircles have been monitored noticeably in the outline.

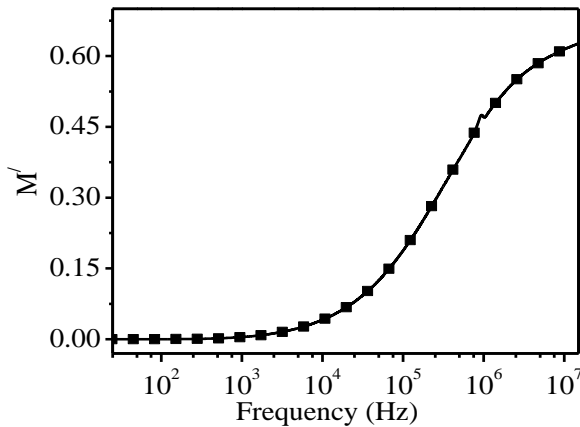


Figure 2(a): Variation of real (M') of electric modulus with frequency for various $\text{Ni}_{0.1}\text{Mn}_{0.4}\text{Cu}_{0.2}\text{Cd}_{0.3}\text{Fe}_2\text{O}_4$

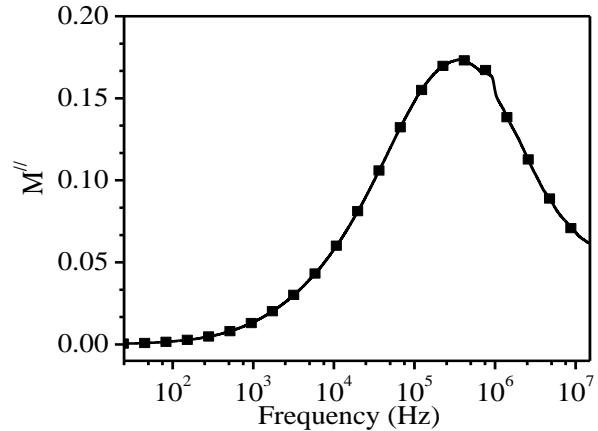


Figure 2(b): Variation of imaginary part (M'') of electric modulus with frequency for various $\text{Ni}_{0.1}\text{Mn}_{0.4}\text{Cu}_{0.2}\text{Cd}_{0.3}\text{Fe}_2\text{O}_4$

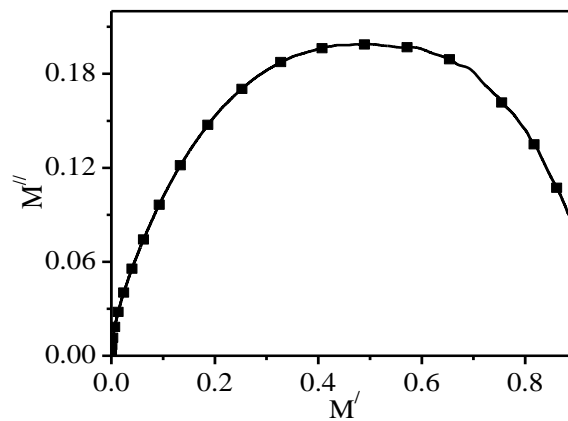


Figure 2(c): Variation of M' vs. M'' of $\text{Ni}_{0.1}\text{Mn}_{0.4}\text{Cu}_{0.2}\text{Cd}_{0.3}\text{Fe}_2\text{O}_4$

3.3. Impedance Spectroscopy

The real (Z') and imaginary (Z'') part of the impedance of $\text{Ni}_{0.1}\text{Mn}_{0.4}\text{Cu}_{0.2}\text{Cd}_{0.3}\text{Fe}_2\text{O}_4$ nano-ferrites with the frequency range 20 Hz to 15 MHz has been given in Figure 3 (a) and Figure 3 (b). The Nyquist impedance plot of the nano ferrites has been given in Figure 3 (c). Using impedance spectroscopy of a ceramic material, it is promising to learn about grain and grain boundary resistance involvement of the materials. The decrease of Z' is inversely connected to the conduction of the substance. Conduction ascends to an explicit frequency, and after that, it turns into invariable. That's why the Z' value gradually decreases, and after an explicit frequency, it demonstrates the least values. In addition, in the low-frequency state, all types of polarization have effects, while, in the high-frequency state, just space charge polarization happens. The

discrepancy in Z'' with frequency has been given in Figure 3 (b). It has been perceived as a climax in Z'' value, and the least value is scrutinized for all the samples as the frequency boosts. From the Cole-Cole plot drawn in Figure 3 (c), the grain and grain boundary resistance value can be resolved. After the extrapolation of Cole-Cole plots, it has been noticed that the acquired semicircles overlies. In the samples, grains operate as the conductive medium, while grain boundary operates as a resistive medium that splits two conductive sheets [16]. Within the impedance spectrum, no third semicircle that originates from the association of the electrode method has been noticed.

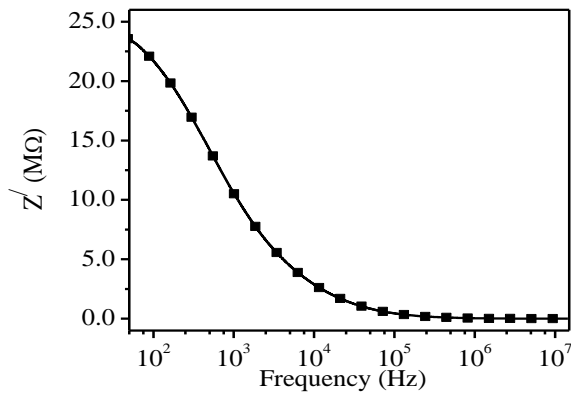


Figure 3(a): Variation of the real part (Z') of impedance with the frequency of $\text{Ni}_{0.1}\text{Mn}_{0.4}\text{Cu}_{0.2}\text{Cd}_{0.3}\text{Fe}_2\text{O}_4$

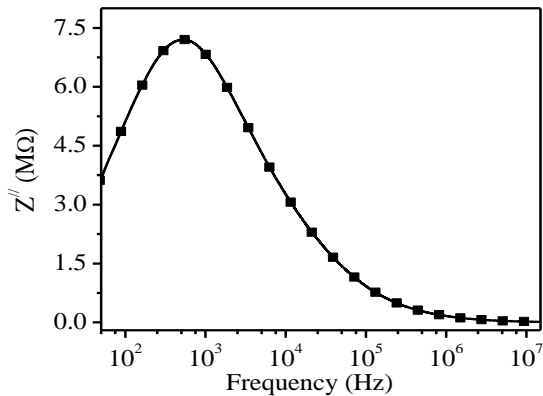


Figure 3(b): Variation of imaginary part (Z'') of impedance with the frequency of $\text{Ni}_{0.1}\text{Mn}_{0.4}\text{Cu}_{0.2}\text{Cd}_{0.3}\text{Fe}_2\text{O}_4$

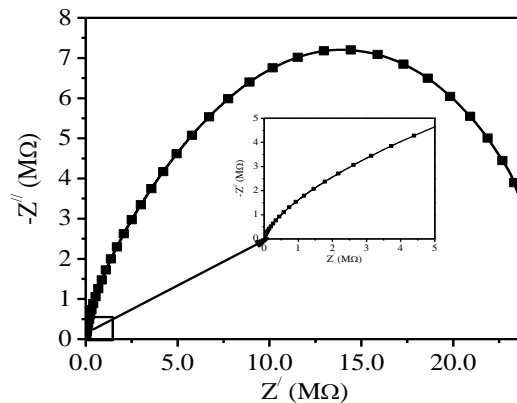


Figure 3(c): The Cole-Cole plot of $\text{Ni}_{0.1}\text{Mn}_{0.4}\text{Cu}_{0.2}\text{Cd}_{0.3}\text{Fe}_2\text{O}_4$

3.4. AC conductivity

AC conductivity (σ_{ac}) can be satisfactorily elucidated by Austin and Mott's polaron hopping model [17]. In agreement with this model, the σ_{ac} value displays straight proportional relation with frequency only for a restricted variety of hopping, while opposite proportional relation with frequency for an extensive variety of polaron hopping. In Figure 4, the discrepancy of σ_{ac} in the frequency from 20 Hz to 15 MHz for all the samples has been given. For ferrite materials, σ_{ac} alters linearly with the augmentation in frequency that is a representative trend. In the current investigation, due to the small polaron hopping, a linear increase in σ_{ac} occurs. With the increase in frequency, electron replacement also boosts that outcome in a linear ascends in ac

conductivity. With the ascend in frequency, the contiguous grains turn into further reactive, then the hopping between two iron states turns into privileged so that σ_{ac} also demonstrate advanced value [18].

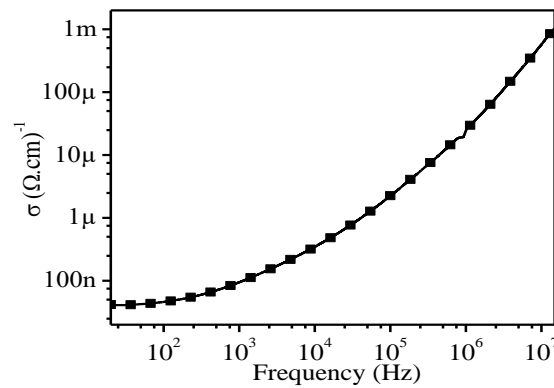


Figure 4: Variation of ac conductivity with the frequency of $\text{Ni}_{0.1}\text{Mn}_{0.4}\text{Cu}_{0.2}\text{Cd}_{0.3}\text{Fe}_2\text{O}_4$

4. Conclusions

Electrical properties play a vital role in proving the suitability of any material for high-frequency applications. The synthesis technique also controls the electrical properties of nano ferrites materials. By facile method sol-gel, auto-combustion procedure has been utilized to synthesis $\text{Ni}_{0.1}\text{Mn}_{0.4}\text{Cu}_{0.2}\text{Cd}_{0.3}\text{Fe}_2\text{O}_4$ nanoparticles. To investigate the suitability of Ni-Mn-Cu-Cd nano ferrites for high-frequency applications, electrical properties have been examined. From the electron-hole hopping method, deviation in dielectric constant can be clarified. The release of space charge contribution causes the minimum M' value in the low-frequency vicinity. Cole-Cole chart of impedance spectroscopy reveals the conduction procedures that take place within the system. It has been viewed from the ac conductivity graph that conductivity enhances linearly with the rise of frequency. Examined properties of $\text{Ni}_{0.1}\text{Mn}_{0.4}\text{Cu}_{0.2}\text{Cd}_{0.3}\text{Fe}_2\text{O}_4$ nanoparticles prove it as a potential applicant for high-frequency applications.

Acknowledgment

The author is grateful to the Department of Physics, Chittagong University of Engineering and Technology (CUET), Chattogram-4349, Bangladesh, for continuous support.

References

- [1]. C. Pereira, A. M. Pereira, C. Fernandes. "Superparamagnetic MFe_2O_4 (M = Fe, Co, Mn) Nanoparticles: Tuning the Particle Size and Magnetic Properties through a Novel One-Step Coprecipitation Route." *Chemistry of Materials*, vol. 24, pp. 1496-504, 2012.
- [2]. H. Igarashi and K. Okazaki. "Effect of Porosity and Grain Size on the Magnetic Properties of Ni-Zn Ferrite." *Journal of the American Ceramic Society*, vol. 60, no. 1-2, pp. 51-54, 1976.
- [3]. E. C. Snelling. "Soft Ferrites, Properties and Applications." 2nd ed., Butter Worth, London, 1988.

- [4]. C. Hu, Z. Gao, X. Yang. "One-pot low temperature synthesis of MFe_2O_4 ($M=Co, Ni, Zn$) superparamagnetic nanocrystals." *Journal of Magnetism and Magnetic Materials*, vol. 320, no.8, pp. L70-L73, 2008.
- [5]. S. Nasrin, F.-U.-Z. Chowdhury, S. M. Hoque. "Study of hyperthermia temperature of manganese-substituted cobalt nano ferrites prepared by chemical co-precipitation method for biomedical application." *Journal of Magnetism and Magnetic Materials*, vol. 479, pp. 126–134, 2019.
- [6]. C. H. Yan, Z. G. Xu, F. X. Cheng, Z. M. Wang, J. D. Sun, C. S. Liao, J. T. Jia. "Nanophased $CoFe_2O_4$ prepared by combustion method." *Solid State Communications*, vol. 111, no.5, pp. 287-291, 1999.
- [7]. K. Mandal, S. P. Mandal, P. Agudo, M. Pal. "A study of nanocrystalline (Mn–Zn) ferrite in SiO_2 matrix." *Applied Surface Science*, vol. 182, pp. 386-389, 2001.
- [8]. Sagar E. Shirsath, B.G. Toksha, R.H. Kadam, S.M. Patange, D.R. Mane, Ganesh S. Jangam, Ali Ghasemi. "Doping effect of Mn^{2+} on the magnetic behavior in Ni–Zn ferrite nanoparticles prepared by sol-gel auto-combustion." *Journal of Physics and Chemistry of Solids*, vol. 71, pp. 1669–1675, 2010.
- [9]. H. Farooq, M. R. Ahmad, Y. Jamil, A. Hafeez, Z. Mahmood, T. Mahmood. "Structural and Dielectric Properties of Manganese Ferrite Nanoparticles." *Journal of Basic & Applied Sciences*, vol. 8, no.2, pp. 597-601, 2012.
- [10]. M. V. Santhosh Kumar, G. J. Shankarmurthy, E. Melagiriappa, K. K. Nagaraja, A. R. Lamani, B. M. Harish. "Dielectric and magnetic properties of high porous Gd^{3+} substituted nickel-zinc ferrite nanoparticles." *Materials Research Express*, vol. 5, no. 4, pp. 046109, 2018.
- [11]. S. P. Yadav, S. S. Shinde, P. Bhatt, S. S. Meena, K. Y. Rajpure. "Distribution of cations in $Co_{1-x}Mn_xFe_2O_4$ using XRD, magnetization and Mössbauer spectroscopy." *Journal of Alloys and Compounds*, vol. 646, pp. 550–556, 2015.
- [12]. C. G. Koops. "On the dispersion of resistivity and dielectric constant of some semiconductors at audio frequencies." *Physical Review*, vol. 83, pp. 121-124, 1951.
- [13]. A. M. Shaikh, S. S. Bellard, B. K. Chougule. "Temperature and frequency-dependent dielectric properties of Zn substituted Li–Mg ferrites." *Journal of Magnetism and Magnetic Materials*, vol. 195, no. 2, pp. 384-390, 1999.
- [14]. M. Kaiser. "Electrical conductivity and complex electric modulus of titanium doped nickel-zinc ferrites." *Physica B: Condensed Matter*, vol. 407, no. 4, pp. 606–613, 2012.
- [15]. T. Prakash, K. P. Prasad, R. Kavitha, S. Ramasamy, B. S. Murty. "Dielectric relaxation studies of nanocrystalline $CuAlO_2$ using modulus formalism." *Journal of Applied Physics*, vol. 102, no. 10, pp. 104104, 2007.
- [16]. A. Behera, N. Mohanty, S. Satpathy, B. Behera, P. Nayak. "Investigation of complex impedance and modulus properties of Nd-doped $_{0.5}BiFeO_{3-0.5}PbTiO_3$ multiferroic Composites." *Open Physics*, vol. 12, no. 12, pp. 851-861, 2014.
- [17]. I. G. Austin, N. F. Mott. "Electrons in disordered structures." *Advanced Physics*, vol. 16, no.61, pp. 49-144, 1967.
- [18]. P. Sivakumar, R. Ramesh, A. Ramanand, S. Ponnusamy, C. Muthamizhchelvan. "Structural, thermal, dielectric and magnetic properties of $NiFe_2O_4$ nanoleaf." *Journal of Alloys and Compounds*, vol. 537, pp. 203–207, 2012.